Estimation of specific reactivities of commercial gel-type resins through modeling the chain sequences distribution

Leandro G. Aguiar, William M. Godoy, Nathália M. Lotufo, Nuno A. B. S. Graça & Alírio E. Rodrigues

Published online: 18 Mar 2024.

Submit your article to this journal ⬈

View related articles ⬈

View Crossmark data ⬈

Taylor & Francis
Taylor & Francis Group

Check for updates

Estimation of specific reactivities of commercial gel-type resins through modeling the chain sequences distribution

Leandro G. Aguiar[a] , William M. Godoy[a], Nathália M. Lotufo[a], Nuno A. B. S. Graça[b], and Alírio E. Rodrigues[b]

[a]Departamento de Engenharia Química, Escola de Engenharia de Lorena, Universidade de São Paulo, Lorena, Brazil; [b]LSRE – Faculdade de Engenharia da Universidade do Porto, Portugal Porto

ABSTRACT

This study evaluates the reactivity of acidic resins through mathematical modeling. To assess the reactivity of resins, a copolymerization model was used, making it possible to estimate chain sequences distribution along their polymeric matrices. A model for the reaction catalyzed by these resins, whose equations were based on power law and molar balances, was coupled to the copolymerization model to describe the whole process. Resin properties were collected from the literature and compared to data provided by the copolymerization model, resulting in a linear correlation between the weighted average chain densities measured by ISEC and the total concentration of sequences between cross-links ($R^2 = 0.988$). The prediction ability of the developed model was compared to a literature approach, which depends on an experimental characterization of the resins by Inverse Steric Exclusion Chromatography (ISEC). Akaike Information Criterion revealed that the models exhibit comparable predictive capabilities, demonstrating that the developed model is able to simulate reactions catalyzed by gel-type resins without requiring equipment for morphology characterization.

Introduction

The application of heterogeneous catalysts in organic reactions has been preferred over homogeneous acid catalysts due to their better recyclability and product isolation, among other advantages. (Chaffey et al. 2021; Farouq and Selim 2023) Specifically, commercial ion-exchange resins have been widely used to catalyze the synthesis of a variety of products, e.g., triethyl citrate by Amberlyst 70® (Bohórquez et al. 2020), solketal by Amberlyst 35® (Corrêa et al. 2022; Faria et al. 2022), and glycerol tertiary butyl ethers by Amberlyst 15® (Bozkurt et al. 2020). Besides these macroreticular resins from the Amberlyst line, gel-type resins, such as Dowex®, are also tested as catalysts in esterification reactions (Erdem and Cebe 2006). Limited information about commercial resins is available, such as ion exchange capacity and cross-linker content, which can be found in the aforementioned references. From the theoretical perspective, studying catalysis with gel-type resins is advantageous due to the reduced number of variables associated with textural properties when compared to macroreticular resins (e.g., negligible internal surface area). This feature allows one to make a close correlation between the polymer network properties of gel-type resins and their catalytic efficiency, which is scarce in the modeling literature. Kinetic models involving adsorption (Rahaman et al. 2015) and intraparticle diffusion (Russo et al. 2020) have been developed for resin-catalyzed reactions and validated with experimental data. Despite the good results provided by these models, the reactivity and accessibility properties of the referred resins as a consequence of their polymerization process can be better explored. In this sense, the kinetics of cross-linking polymerization play an important role on the prediction of features of a polymer matrix (Sims 2021; Tobita 2021). Studies on the evolution of

---

cross-links concentration (Likozar 2011; Likozar and Krajnc 2011) as well as the combined approach Kinetics/Transport Phenomena have been carried out for cross-linking of polymers. These studies are important steps toward the description of polymer network properties and their use in different applications. Inverse steric exclusion chromatography (ISEC) has been employed to assess the chain density distribution of ion-exchange resins. This technique consists of identifying and quantifying different densities in a discretized way. In general, the chain densities are divided into five zones: 0.1, 0.2, 0.4, 0.8 and 1.5 nm nm^{-3}. In ISEC, the investigated materials are used as stationary phase in a chromatographic column and elution volumes of standard solutes with known molecular size are measured (Jeřábek et al. 2002; Bringué et al. 2019). The advantage of this characterization is that a detailed catalytic study can be carried out, defining a reactivity for each region of the catalyst. However, five parameters (one for each region) need to be adjusted in this kind of model, and the experimental characterization of the resins must be performed. Recently, a copolymerization model that provides information on the cross-link density of ion exchange resins was developed (Aguiar et al. 2021). This model estimates a fraction of inaccessible catalytic sites in a given resin based on its chain sequences distribution (CSD). In the present study, a refined model is proposed in which a variable reactivity as a function of CSD is considered. The novelty of this improved model relies on considering that the reactivity will tend to zero in the densest zones where catalytic sites are practically inaccessible, and will be maximum (pseudo-homogeneous assumption) in the least dense zones.

Mathematical model development

Two mathematical models were tested with literature data obtained from catalytic experiments. Both models were described by following the assumptions:

- Power law rate equation
- Mass transfer resistances were considered to be negligible

- Uniform distribution of catalyst particles throughout the reaction medium
- Isothermal reaction

The detailed model equations are described in the following sections.

Specific activity as a function of chain density (SACD model)

This model considers different reactivities along the catalytic resin. The model fitting is conducted through a multiple regression of five reactivities, one for each region of the catalyst, as reported in the literature (Jeřábek et al. 2002). To apply this model, it is mandatory to characterize the catalytic resin in terms of swollen-state morphology by using the Inverse Steric Exclusion Chromatography (ISEC) method. Then, the reaction rate (r) is calculated through Equation (1) (Jeřábek et al. 2002).

$$r = \sum_{i=0.1}^{1.5} R_i V_i \qquad (1)$$

Where r is in mmol h^{-1} g^{-1}, R_i is the specific activity of the polymer fraction with chain density C_i (with $C_i = 0.1, 0.2, 0.4, 0.8$ or 1.5) in mmol h^{-1} mL^{-1}, and V_i is the volume that the fraction i occupies in 1 g of resin (mL g^{-1}). In Equation (1), the index i represents the five distinct regions with different C_i values, meaning that this summation consists of five terms. In this approach, Jeřábek et al. (2002) experimentally determined the values of r for various resins. The volume fractions with chain densities of 0.1, 0.2, 0.4, 0.8, and 1.5 were assessed using ISEC. Subsequently, a regression analysis employing the experimental data and Equation (1) was performed to derive the specific activities R_i.

Due to the plenty of studies on organic reversible reactions (e.g., esterification) catalyzed by commercial resins, the generic reaction represented in Equation (2) was considered.

$$A + B \rightleftarrows C + D \qquad (2)$$

Where A, B, C and D may represent acid, alcohol, ester and water, respectively (considering an esterification).

Considering the aforementioned reaction in presence of a solid catalyst, the reaction rate can be written in terms of a power law, as follows.

$$(-r_A) = k[IEC]C_{Cat}\left(C_A C_B - \frac{C_C C_D}{K_{eq}} \right) \quad (3)$$

The term $(-r_A)$ in Equation (3) is equivalent to the term r in Equation (1), with the key distinction lying in the available data for calculation. $(-r_A)$ is computed using power law kinetics (when concentrations and kinetic constants are available), while r is determined from morphology data, including specific activity and volume fractions.

Where $(-r_A)$ is the consumption rate of the reagent A (mol L^{-1} h^{-1}), k is the rate coefficient (L^2 mol^{-2} h^{-1}), $[IEC]$ is the ion exchange capacity of the resin (mol g^{-1}), C_{Cat} is the catalyst concentration (g L^{-1}), K_{eq} is the equilibrium constant and C_A to C_D are the concentrations of compounds (mol L^{-1}). Details regarding the ion exchange capacities (IEC) of the resins along with their corresponding references are outlined in Table 1. The equilibrium constant (K_{eq}) values utilized in the simulations were sourced from the literature (Aguiar et al. 2021).

The Equation (3) takes into account the pseudo-homogeneous hypothesis, which is reasonable for styrene-divinylbenzene catalysts in organic media, due to the considerable particle swelling and low mass transfer resistance.

The parameter k takes into account the reactivities in all chain densities along the resin, and can be written as:

$$k = \sum_{i=0.1}^{1.5} k_i \frac{V_i C_i}{\sum_{s=0.1}^{1.5} V_s C_s} \quad (4)$$

The variable k_i represents the rate coefficient associated with the polymer chain density for different values of C_i (L^2 mol^{-2} h^{-1}). Where C_i is defined as 0.1, 0.2, 0.4, 0.8, 1.5. Therefore, 5 parameters ($k_{0.1}$, $k_{0.2}$, $k_{0.4}$, $k_{0.8}$, $k_{1.5}$) were fitted in the SACD Model. The best fittings were obtained by minimizing the sum of squared errors (SSE) between the model and experimental data.

Specific activity as a function of sequence lengths (SASEQ model)

The SASEQ Model employs a copolymerization approach to predict cross-linking information regarding the resins, as described in a previous work (Aguiar et al. 2021). To estimate this cross-linking data, the model considers the standard batch copolymerization of styrene with divinylbenzene (DVB), initiated by benzoyl peroxide (1 mol%), conducted at 150% dilution of monomers in the organic phase and 90 °C for 30 h, as described by Coutinho et al. (2006). This choice is made due to the confidential nature of the procedures for producing commercial resins. These selected conditions and synthesis procedures,

Table 1. Resins properties.

| Resin	DVB (%)	IEC (mmol g^{-1})	S_A (m^2 g^{-1})	V_{Pores} (mL g^{-1})	D_{Pore} (A)	D_{Part} (mm)	Reference
Amberlyst 15 (A15)	20	4.81	55.0	0.622	265	0.740	(Iborra et al. 2000; Casas et al. 2011; Guilera et al. 2015)
Amberlyst 16 (A16)	12	4.80	35.0	1.136	–	0.700	(Dixit and Yadav 1996; Casas et al. 2011; Guilera et al. 2015)
Amberlyst 35 (A35)	20	5.23	35.7	0.504	–	0.660	(Dos Reis et al. 2005; Casas et al. 2011; Tejero et al. 2016)
Amberlyst 36 (A36)	12	5.40	33.0	1.261	240	0.630	(Rodriguez and Setínek 1975; Dos Reis et al. 2005; Casas et al. 2011; Tejero et al. 2016)
Amberlyst 39 (A39)	8	5.00	1.1	1.643	176	0.710	(Casas et al. 2011; Komoń et al. 2013; Guilera et al. 2015; Tejero et al. 2016)
Dowex 50Wx2 (D2)	2	4.83	6.9	2.677	85	0.223	(Dosuna-Rodríguez and Gaigneaux 2012; Guilera et al. 2015)
Dowex 50Wx4 (D4)	4	4.95	–	1.920	–	0.570	(Casas et al. 2011; Guilera et al. 2015)
Dowex 50Wx8 (D8)	8	4.83	2.4	1.404	26	0.111	(Rodriguez and Setínek 1975; Ali and Merchant 2009; Guilera et al. 2015)
Purolite CT224	4	5.34	–	1.859	–	0.320	(Casas et al. 2011; Tejero et al. 2016)
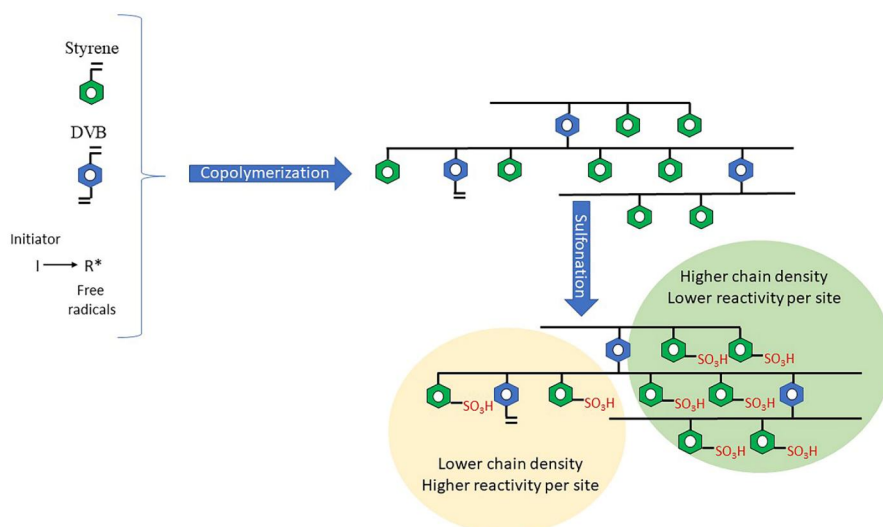
Figure 1. Scheme of the resin synthesis steps.

involving copolymerization followed by sulfonation, were deemed suitable since the resulting resins exhibit properties (e.g., ion exchange capacity) closely resembling those of commercial resins. Additionally, it was assumed that the sulfonation procedure does not significantly alter the conformation of the chains along the resin but incorporates sulfonic groups into it.

A scheme of the production and characteristics of a sulfonated resin is illustrated in Figure 1.

The details about these preliminary simulations for different DVB feedings can be found elsewhere (Aguiar et al. 2021). The referred copolymerization model provides sequences distributions which characterize the chain densities along the synthesized resin. In the present approach, the term sequence represents a number of repeating units n connecting two groups that are present in the polymerization process. In the study of Aguiar et al. (2021), 5 kinds of sequences are defined, and the type of interest in this work is the sequence L_{En}, which is a sequence containing n styrene units connecting two cross-link points in the polymer network. Figure 2 illustrates the final distributions (at the end of the copolymer synthesis) of fractions of L_{En} sequences ($Y_{LE,n}$) for different DVB feed rates used in copolymerization process.

It is understood that the shorter the sequence, the greater the influence of steric effects in the surroundings of this sequence. In terms of application in catalysis, the accessibility to catalytic sites
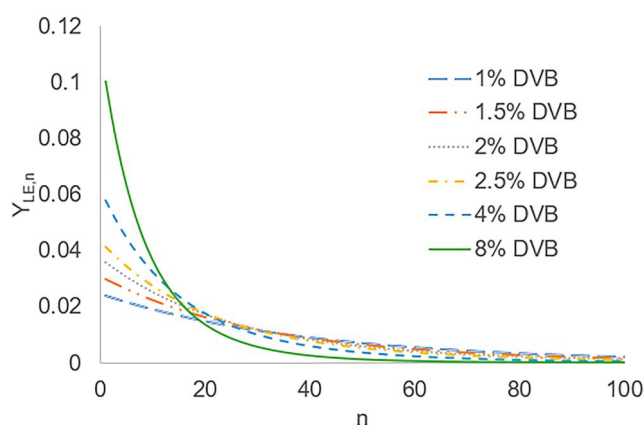

Figure 2. Final distribution $Y_{LE,n}$ for different DVB contents. Simulation conditions: 1% (mol) benzoyl peroxide at 150% dilution and 90 °C for 30 h.

decreases as the value of n, in the sequence L_{En} is reduced. On the other hand, as the sequence is increased, the accessibility to catalytic sites also increases, and a limit is proposed (n_{lim}), from which it is assumed that there is no more accessibility restriction, i.e., the reactivity of catalytic sites located in sequences L_{En}, with $n \geq n_{lim}$, becomes constant (Figure 3). The balance of sequences and additional information on the copolymerization model can be found in the Supporting Information.

In Figure 3, the sulfonated unit is an aromatic ring with a sulfonic group attached to it, which has the ability of an acidic catalytic site. A correlation between the reactivity and n must be defined for the sequences with $n < n_{lim}$. The present work focused on the study of gel-type resins as catalysts. Hence, the results from the work of
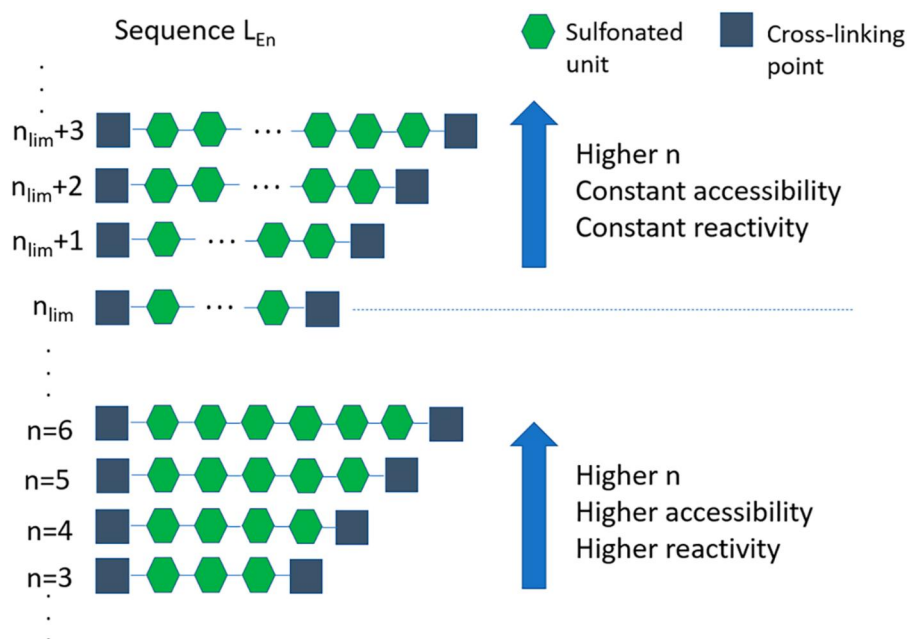
Figure 3. Pictorial representation of the SASEQ model.

Jeřábek et al. (2002) and Aguiar et al. (2021), in which only gel-type resins were tested, were used to determine the referred correlation. The reactivity data obtained by Jeřábek et al. (2002) for the different polymer chain densities (C) are plotted in Figure 4.

Jeřábek et al. (2002) states that the range of densities of swollen polymer mass detectable by ISEC spans from 0.1 (representing an extremely swollen polymer matrix with a density approaching that of the polymer coil of dissolved uncrosslinked polymer) to 1.5 $nm\,nm^{-3}$ (dense network, poorly accessible even for the smallest molecules due to the absence of enthalpic interactions). Consequently, in zones with higher polymer chain densities, lower specific activities are expected, as observed by Jeřábek et al. (2002) (dots in Figure 4). As observed, the data points in Figure 4 can be reasonably fitted with an exponential function. The aim of this fitting was to estimate the specific reactivity in relation to the polymer chain density using a minimal number of parameters (e.g., 2). It was determined that an exponential curve offers a superior fit compared to other elementary functions such as linear, polynomial, and power functions. Since, in the SASEQ Model, the polymer chain density is represented by the sequences L_{En}, an exponential function for the rate coefficient k, depending on
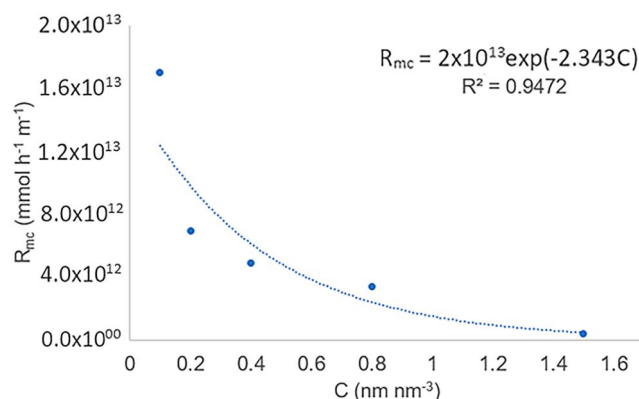

Figure 4. Correlation between specific reactivity for Bisphenol A synthesis per unit of polymer chain length (r_{mc}) and the polymer chain density (C).

n, is proposed, as written in Equation (5).

$$k = k_0 \left(\sum_{n=1}^{n_{lim}-1} a\,exp\left(\frac{b}{n}\right) Y_{LEn} + \sum_{n=n_{lim}}^{200} Y_{LEn} \right) \quad (5)$$

The power law was also considered in the SASEQ Model. So, substituting Equation (5) in Equation (3):

$$(-r_A) = k_0 \left(\sum_{n=1}^{n_{lim}-1} a\,exp\left(\frac{b}{n}\right) Y_{LEn} + \sum_{n=n_{lim}}^{200} Y_{LEn} \right) [IEC]C_{Cat}$$
$$\left(C_A C_B - \frac{C_C C_D}{K_{eq}} \right)$$
$$(6)$$

Where a, b and n_{lim} are adjustable parameters related to the reactivity variation (see Figure 3),

k_0 is the maximum rate coefficient, i.e., considering the absence of steric effects (adjustable for a given reaction), and Y_{LEn} is the fraction of the sequence L_{En} in relation to the sum of all sequences from $n = 1$ to $n = 200$. The concentration of sequences with $n > 200$ is very close to zero and was neglected in this study. The parameters a and b define the shape of the exponential reactivity variation, which can vary depending on the resin and the characteristics of the reaction medium. Given that reactivity is anticipated to increase with higher values of n, negative values of b are expected. The parameter $n_{\lim}$, serving as the dividing line in sequence length, demarcates two distinct behaviors: variable reactivity (for $n < n_{\lim}$) and constant reactivity (for $n > n_{\lim}$).

Therefore, 4 parameters (a, b, $n_{\lim}$ and k_0) were fitted in the SASEQ Model. The best fittings were obtained by minimizing the SSE between the model and experimental data.

A comparison of models was made based on Akaike Information Criterion (Al-Rubaie et al. 2007) as described in Equations (7) and (8).

$$AIC = Nln\left(\frac{SSE}{N}\right) + 2K \tag{7}$$

$$AIC_C = AIC + \frac{2K(K+1)}{N - K - 1} \tag{8}$$

where AIC: Akaike information criterion; AIC_C: Akaike Information Criterion corrected for small samples; N: Number of data points; K: Number of model parameters; SSE: Sum of Squared Errors.

According to Al-Rubaie et al. (2007), the smallest AIC_C among all candidate models is referred to as the best model, taking into account SSE, number of parameters, and number of data points.

Results and discussion

As mentioned in the preceding section, the SACD model relies on a kinetic study previously employed (Jeřábek et al. 2002; Badia et al. 2015). This model requires the fitting of 5 parameters and depends on an equipment to analyze the swollen morphology of the resins. Conversely, the SASEQ Model, developed herein, requires the fitting of 4 parameters and does not depend on any experimental characterization of the resins. The variation in reactivity along the catalyst can be estimated with the information provided by the copolymerization model. Figure 5 shows a comparison between both models and the experimental reaction rate data for Bisphenol A sinthesis provided by Jeřábek et al. (2002).

Figure 5 displays measurements performed in a CSTR reactor, specifically focusing on low acetone conversions ($<10\%$). Within this range, the observed reaction rates are regarded as independent of conversion, serving as a reliable measure of the catalytic activity exhibited by the resins (Jeřábek et al. 2002). The experiments were conducted at $70\,°C$ and with a phenol/acetone molar ratio of 8:1. The experimental reaction rates, as shown in Figure 5, were obtained for gel-type styrene-divinylbenzene sulfonated resins with DVB content within the range of 1% to 8%, encompassing a total of 7 data points. Higher reaction rates are obtained as the DVB content in the resin is reduced, since resins with low DVB percentages are more flexible, allowing a better accessibility to the catalytic sites in the reaction medium (Tejero et al. 2016). It can be observed that both models provided good predictions.

Erdem and Cebe (2006) studied the esterification of propionic acid with n-amyl alcohol also catalyzed by gel-type resins. The tested resins are from the commercial line Dowex® and contain 2, 4, and 8% DVB (namely D2, D4, and D8, respectively). All resins were applied to the same reaction conditions and compared, as shown in Figure 6.

It can be verified that both models present very similar results for the esterification of
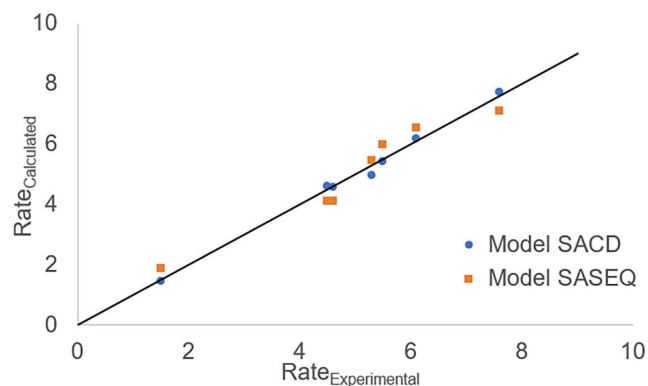

Figure 5. Reaction rates of Bisphenol A synthesis (mmol h^{-1} g^{-1}). A comparison between experimental and model data for gel-type styrene-divinylbenzene sulfonated resins at DVB percentages of 1%, 1.5%, 2%, 2.5%, 4%, 4%, and 8%. The graph illustrates an increasing trend in reaction rates as DVB percentage decreases.

propionic acid with n-amyl alcohol on the referred Dowex resins. The conversion profile is increased as the DVB content is reduced, as expected for gel-type resins. This behavior was well represented by models SACD and SASEQ. The good predictability of both models for reactions catalyzed by gel-type resins is justifiable, the DVB content (and consequently the chain density) can be considered the only factor that affects the reactivity of the resin. In other words, variables such as porosity, surface area, and pore diameter, which would considerably affect the reaction rate, can be neglected in this kind of catalyst. In order to verify the ability of the models to predict the results of reactions catalyzed by resins of different kinds, simulations with data from the esterification of levulinic acid with butanol catalyzed by gel-type and macroporous resins were carried out (Tejero et al. 2016). The results are presented in Figure 7.

The gel-type resins used in the work of Tejero et al. (2016) were D2, D4, D8 (Dowex), and Purolite CT224, all in the range 2–8% DVB. Similarly to the fitting obtained in Figure 6, a good agreement between models and experimental data was obtained for the reaction catalyzed by gel-type resins (Figure 7a,b), with R^2 of 0.96 and 0.94 respectively. The previous model developed by our research group, the Inaccessible Sites Model (ISM) (Aguiar et al. 2021), was also applied to the experiments conducted with gel-type resins in Tejero et al.'s work (2016), yielding an R^2 of 0.92. The ISM posits the existence of a fraction of inaccessible sulfonated units, denoted as Y_{ISU}, which are unavailable for catalysis. This parameter is a function of the chain density of each resin.

In the current study, we have enhanced the model by considering the gradual variation of reactivity across different polymer zones and introducing a limit on sequence length beyond which reactivity remains constant. This limit is a crucial piece of information because it depends on the size of the reacting molecules in the catalyzed reaction, a factor not accounted for in the ISM model.

Despite the ISM model's simplicity, with only two parameters (the rate constant k and Y_{ISU}), it is found to be less suitable than the SASEQ Model when applied to the data from Tejero et al. (2016). This conclusion is supported by the Akaike criterion (see footnotes of Table 3).

On the other hand, catalysis with macroporous resins (A15, A16, A35, A36, and A39 from Amberlyst®) was simulated, and poor fittings were obtained (Figure 7c,d). It is understood that transport phenomena must be taken into account in order to build a model for catalysts with considerably large surface areas, i.e., the larger the surface area, the higher the mass transfer rate from the macropores to the gel region of the resin. The contrast between the properties of gel-type and macroporous resins studied herein can be verified in Table 1. Since the present models do not take into account transport phenomena, they are applicable only to gel-type resins, which explains the poor fittings observed in Figure 7c,d.

It can be evidenced that SASEQ Model represents well only catalysis with gel-type resins by correlating information about sequences L_{En}
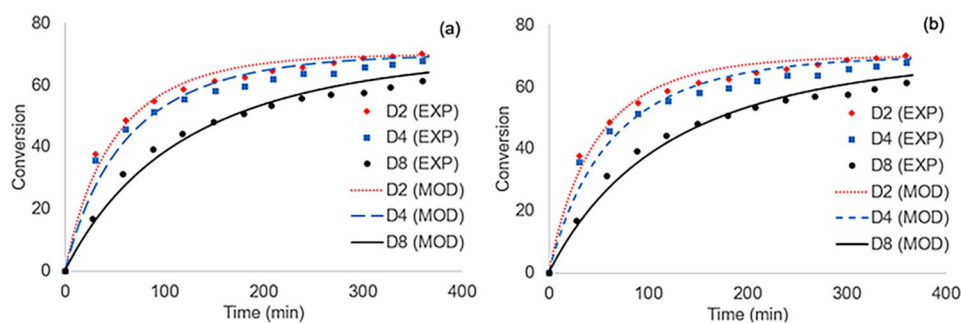

Figure 6. Fittings with data from Erdem and Cebe (2006). (Erdem and Cebe 2006) (a) SACD model, (b) SASEQ model. EXP: Experimental data, MOD: Model predictions. $K_{eq} = 5.44$ (Aguiar et al. 2021). Experimental conditions: $T = 333K$, $C_A = C_B = 5.02$ mol L^{-1}, $C_{Cat} = 90.35$ g L^{-1}. D2, D4 and D8 are Dowex® resins with 2, 4 and 8% DVB respectively.
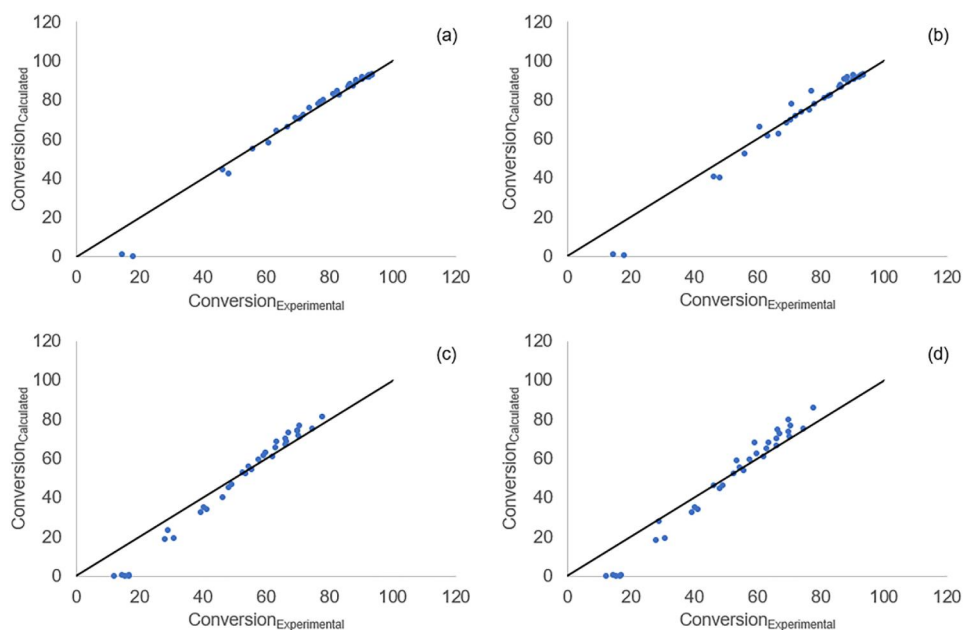
Figure 7. Fittings with conversion data from tejero et al. (Tejero et al. 2016) Upper graphs: (a) SACD model for gel-type resins, (b) SASEQ model for gel-type resins. Bottom graphs: (c) SACD model for macroporous resins, (d) SASEQ model for macroporous resins. $K_{eq} = 6.596$ (Aguiar et al. 2021). Experimental conditions: $T = 353K$, $C_A = 2.656$ mol L^{-1}, $C_B = 7.968$ mol L^{-1}, $C_{Cat} = 7.143$ g L^{-1}. The points represent conversions at different reaction times.

(from the copolymerization model) with the polymer chain densities obtained from ISEC analysis. Figure 8 presents a correlation between the sum of all sequences L_{En} (with $n_{max} = 100$ (Aguiar et al. 2021)) and the weighted average polymer chain density (C_m). The values of C_m were calculated through Equation (9), as follows.

$$C_m = \sum_{i=0.1}^{1.5} C_i f_{Vi} \qquad (9)$$

where $f_{Vi} = \dfrac{V_i}{\sum_{i=0.1}^{1.5} V_i}$.

It is important to emphasize that the present copolymerization model is not able predict how the chain sequences are spatially arranged, i.e., the chain density distribution has not been estimated. A linear correlation can be observed in Figure 8a, indicating that the copolymerization model is able to predict with good accuracy the average chain density of gel-type resins. On the other hand, the present copolymerization model does not take into account the heterogeneities caused by the presence of a porogen agent, which results in an incorrect description of the chain sequences distribution for macroporous resins, as can be seen in Figure 8b. Therefore, the SASEQ Model (jointly with the copolymerization model) is a powerful tool to simulate reactions catalyzed

Table 2. Parameters fitted in the models.

Model	Parameter*	Erdem**	Tejero (gel)**	Tejero (macro)**
SACD	$k_{0,1}$	0	0	13.586
	$k_{0,2}$	0.912	7.474	0
	$k_{0,4}$	0.200	1.843	159.876
	$k_{0,8}$	0.517	2.502	2.438
	$k_{1,5}$	0.032	0.794	0.774
SASEQ	k_0	0.337	2.435	2.228
	a	20.531	19.065	3869.556
	b	−57.710	−62.264	−50.710
	n_{lim}	49	50	7

*k_0 and $k_{0,1}$ to $k_{1,5}$ in L^2 mol^{-2} h^{-1}. **Data fitted in Figures 6 and 7: Erdem (Erdem and Cebe 2006), Tejero (Tejero et al. 2016).

by gel-type resins without the need to conduct morphology characterization. The use of the balance of sequences to estimate the morphology of these resins proved useful, as shown in Figure 7 and corroborated by Figure 8.

Table 2 lists the values of the parameters fitted in both models.

In a previous work (Aguiar et al. 2021), a model that divided the catalytic sites only into accessible and inaccessible (ISM) provided $k = 9 \times 10^{-5}$ L^2 mol^{-2}s^{-1} for the data from Erdem and Cebe (2006) and $k = 5.5 \times 10^{-4}$ L^2 mol^{-2} s^{-1} for the data from Tejero et al. (2016) (Experimental conditions provided in the captions of Figures 6 and 7). These values are close to the values found for k_0 in the SASEQ Model, which represent the maximum reactivity inside the resin, i.e., there is

Table 3. Akaike Information Criterion For models comparison.

Reference data	SSE SACD	SSE SASEQ	AIC_C SACD	AIC_C SASEQ
Jerabek (Jeřábek et al. 2002)	0.154	1.281	35.940	8.763
Erdem (Erdem and Cebe 2006)	8.573	8.646	−21.217	−23.529
Tejero (Gel) (Tejero et al. 2016)	16.838	23.209	6.292	14.439
Tejero (Macro) (Tejero et al. 2016)	44.801	50.631	45.540	48.092

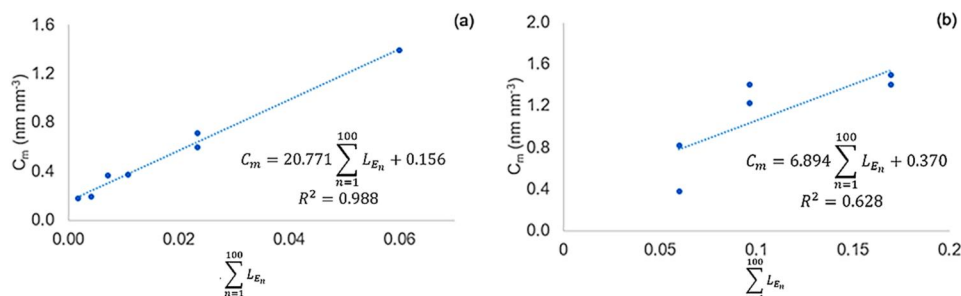ISM fittings provided $AIC_C = 19.637$ for Tejero (Gel) data.

Figure 8. Correlation between measured (Y axis) and simulated (X axis) chain density data for (a) gel-type resins (1%, 1.5%, 2%, 2.5%, 4%, 4%, and 8% DVB) based on jeřábek et al. (Jeřábek et al. 2002), and (b) macroporous resins (8%, 8%, 12%, 12%, 20%, and 20% DVB) from tejero et al. (Tejero et al. 2016) In both cases, c_m exhibits an increasing trend with the rise in DVB percentage.

an agreement between the different approaches. Erdem and Cebe (2006) estimated a rate coefficient of 4.9×10^{-5} L^2 $mol^{-2}s^{-1}$ for the esterification of propionic acid with n-amyl alcohol at 333 K. This value is lower in comparison to the k_0 provided by the SASEQ Model ($k_0 = 9.37 \times 10^{-5}$ L^2 $mol^{-2}s^{-1}$). This difference can be attributed to the hindering effects induced by the varying chain densities within the resin, a factor that was not considered in Erdem and Cebe's study. The zeros fitted for some parameters in the SACD model are related to a chain density that was not present in the resins (e.g., $V_{0,1} = 0$ for D2, D4 and D8). In Table 2, the parameters a, b and n_{lim} fitted for Erdem are similar to the values fitted for Tejero (gel), evidencing again the ability of SASEQ Model to describe catalytic data provided by gel-type resins. This similarity emphasizes the standard behavior of gel-type resins; and indicates that, in the polymer matrix, more than 50 repeating units between cross-linking points are necessary to avoid accessibility limitations to catalytic sites for the studied reactions. On the other hand, for the macroporous resins, the values of the fitted parameters did not present reasonable coherence, as expected.

Table 3 shows a comparison of models through Akaike Information Criterion.

According to Al-Rubaie et al. (2007), the lowest AIC_C value indicates which is the best model, taking into account the number of data points, parameters, and the sum of squared errors (SSE). Comparing AIC_C of the models SACD and SASEQ, it can be concluded that they are quite equivalent. However, in terms of practical application, the SASEQ Model has the advantage of not requiring equipment for morphology, as it is able to provide an estimate of the chain density of the polymeric catalyst.

Conclusion

A mathematical model for organic reactions catalyzed by sulfonated styrene-divinylbenzene resins was developed and validated with experimental data. A copolymerization model based on the balance of sequences was used to provide information on the morphology of the resins, which presented a linear correlation with the weighted average chain densities measured by ISEC, with $R^2 = 0.988$. The model here developed (SASEQ) proved equivalent to the literature approach (SACD). However, SASEQ Model does not require characterization equipment to determine the resin morphology (ISEC), which is an advantage over SACD model. The rate coefficients obtained in this modeling study are coherent in comparison with literature data, and the other parameters were consistent for the same type of resin. In terms of accessibility restrictions along the polymer matrix,

a limit of 50 repeating units between cross-linking points was found, beyond which no reactivity variation is expected to occur. Finally, model fitting attempts with data from reaction catalyzed by macroporous resins did not provide good agreement with experimental data, i.e., the developed model is able to represent only catalysis with gel-type resins. Future studies involving mass transfer parameters and a multiphase system can be carried out from this work.

Disclosure statement

No potential conflict of interest was reported by the author(s).

Symbology

a and b	Adjustable parameters related to reactivity variation
AIC	Akaike Information Criterion
AIC_C	Akaike Information Criterion corrected for small samples
C_A to C_D	Concentrations of compounds (mol L^{-1})
C_{Cat}	Catalyst concentration (g L^{-1})
C_i	Polymer chain density (nm nm^{-3})
C_m	Average polymer chain density (nm nm^{-3})
CSD	Chain sequences distribution
DVB	Divinylbenzene
D2	Dowex resin with 2% of DVB
D4	Dowex resin with 4% of DVB
D8	Dowex resin with 8% of DVB
f_{Vi}	Fraction of polymer chains with volume V_i
IEC	Ion exchange capacity of the resin (mol g^{-1})
ISEC	Inverse steric exclusion chromatography
ISM	Inaccessible sites model
k	Rate coefficient $(\text{L}^2 \text{mol}^{-2} \text{ s}^{-1})$
k_0	Maximum rate coefficient $(\text{L}^2 \text{ mol}^{-2} \text{ s}^{-1})$
K	Number of model parameters
K_{eq}	Equilibrium constant
L_{En}	Sequence with n styrene units connecting two cross-linking points in the polymer network
n	Number of repeating units in a sequence
$n_{\lim}$	Limit for the number of repeating units in a sequence
$n_{\max}$	Maximum number of repeating units in a sequence
N	Number of data points
$(-r_A)$	Consumption rate of the reagent A $(\text{mol L}^{-1} \text{ h}^{-1})$
R_i	Specific activity of the polymer fraction with chain density C_i $(\text{mmol h}^{-1} \text{ mL}^{-1})$
r	Reaction rate $(\text{mol L}^{-1}\text{s}^{-1})$
SACD	Specific activity as a function of chain density
SASEQ	Specific activity as a function of sequences lengths
SSE	Sum of Squared Errors
V_i	Volume fraction of chains with density C_i (mL g^{-1})
V_s	Volume fraction of chains with density C_S (mL g^{-1})
Y_{ISU}	Fraction of inaccessible sulfonated units
Y_{LE_n}	Fraction of the sequence L_{E_n}

ORCID

Leandro G. Aguiar (iD) http://orcid.org/0000-0002-2055-9317

References

Aguiar LG, Godoy WM, Nápolis L, Faria RPV, Rodrigues AE. 2021. Modeling the effect of cross-link density on resins catalytic activities. Ind Eng Chem Res. 60(17): 6101–6110. doi:10.1021/acs.iecr.1c00695.

Aguiar LG, Gonçalves MAD, Pinto VD, Dias RCS, Costa M, Giudici R. 2014. Mathematical modeling of NMRP of styrene-divinylbenzene over the pre- and post-gelation periods including cyclization. Macro Reaction Engineering. 8(4): 295–313. doi:10.1002/mren.201300171.

Ali SH, Merchant SQ. 2009. Kinetic study of dowex 50 Wx8-catalyzed esterification and hydrolysis of benzyl acetate. Ind Eng Chem Res. 48(5):2519–2532. doi:10.1021/ie8006787.

Al-Rubaie KS, Godefroid LB, Lopes JAM. 2007. Statistical modeling of fatigue crack growth rate in Inconel alloy 600. Int J Fatigue. 29(5):931–940. doi:10.1016/j.ijfatigue.2006.07.013.

Badia JH, Fité C, Bringué R, Iborra M, Cunill F. 2015. Catalytic activity and accessibility of acidic ion-exchange resins in liquid phase etherification reactions. Top Catal. 58(14–17):919–932. doi:10.1007/s11244-015-0460-3.

Bohórquez WF, Osorio-Pascuas OM, Santaella MA, Orjuela A. 2020. Homogeneous and heterogeneous catalytic kinetics in the production of triethyl citrate. Ind Eng Chem Res. 59(43):19203–19211. doi:10.1021/acs.iecr.0c03690.

Bozkurt ÖD, Bağlar N, Çelebi S, Uzun A. 2020. Screening of solid acid catalysts for etherification of glycerol with isobutene under identical conditions. Catal Today. 357: 483–494. doi:10.1016/j.cattod.2019.07.025.

Bringué R, Ramírez E, Iborra M, Tejero J, Cunill F. 2019. Esterification of furfuryl alcohol to butyl levulinate over ion-exchange resins. Fuel. 257:116010. doi:10.1016/j.fuel.2019.116010.

Casas C, Bringué R, Ramírez E, Iborra M, Tejero J. 2011. Liquid-phase dehydration of 1-octanol, 1-hexanol and 1-pentanol to linear symmetrical ethers over ion exchange resins. Appl Catal A Gen. 396(1-2):129–139. doi:10.1016/j.apcata.2011.02.006.

Chaffey DR, Bere T, Davies TE, Apperley DC, Taylor SH, Graham AE. 2021. Conversion of levulinic acid to levulinate ester biofuels by heterogeneous catalysts in the presence of acetals and ketals. Appl Catal B. 293:120219. doi: 10.1016/j.apcatb.2021.120219.

Corrêa I, Faria RPV, Rodrigues AE. 2022. Continuous valorization of glycerol into solketal: from the fixed-bed adsorptive reactor to the simulated moving-bed reactor. Ind Eng Chem Res. 61(11):4017–4030. doi:10.1021/acs.iecr.1c04832.

Coutinho FMB, Rezende SM, Soares BG. 2006. Characterization of Sulfonated Poly (Styrene-Divinylbenzene) and Poly-(Divinylbenzene) and Its Application as Catalysts in Esterification Reaction. J. Appl. Polym. Sci. 102(4):3616–3627.

Dixit AB, Yadav GD. 1996. Deactivation of ion-exchange resin catalysts. Part I: alkylation of o-xylene with styrene. Styrene React Funct Polym. 31(3):237–250. doi:10.1016/1381-5148(96)00062-4.

Dos Reis SCM, Lachter ER, Nascimento RSV, Rodrigues JA, Jr., Reid MG. 2005. Transesterification of Brazilian Vegetable Oilswith Methanol over Ion-Exchange Resins. J Americ Oil Chem Soc. 82(9):661–665. doi:10.1007/s11746-005-1125-y.

Dosuna-Rodríguez I, Gaigneaux EM. 2012. Glycerol acetylation catalysed by ion exchange resins. Catal Today. 195(1):14–21. doi:10.1016/j.cattod.2012.04.031.

Erdem B, Cebe M. 2006. Kinetics of esterification of propionic acid with n-amyl alcohol in the presence of cation exchange resins. Korean J Chem Eng. 23(6):896–901. doi:10.1007/s11814-006-0005-3.

Faria RPV, Gonçalves JC, Corrêa I, Ribeiro AM, Rodrigues AE. 2022. Improving the performance of a simulated moving bed reactor for the synthesis of solketal by implementing multifeed strategy. Ind Eng Chem Res. 61(39):14531–14545. doi:10.1021/acs.iecr.2c01352.

Farouq R, Selim Y. 2023. Functionalized polyethylene glycol as a catalyst for esterification of salicylic acid. J Polym Environ. 31(6):2285–2293. doi:10.1007/s10924-022-02754-1.

Guilera J, Ramírez E, Fité C, Tejero J, Cunill F. 2015. Synthesis of ethyl hexyl ether over acidic ion-exchange resins for cleaner diesel fuel. Catal Sci Technol. 5(4):2238–2250. doi:10.1039/C4CY01548G.

Iborra M, Tejero J, Cunill F, Izquierdo JF, Fité C. 2000. Drying of acidic macroporous styrene-divinylbenzene resins with 12-20% cross-linking degree. Ind Eng Chem Res. 39(5):1416–1422. doi:10.1021/ie9904807.

Jeřábek K, Hanková L, Prokop Z, Lundquist EG. 2002. Relations between morphology and catalytic activity of ion exchanger catalysts for synthesis of bisphenol A. doi: 10.1016/S0926-860X(02)00099-6.

Komoń T, Niewiadomski P, Oracz P, Jamróz ME. 2013. Esterification of acrylic acid with 2-ethylhexan-1-ol: thermodynamic and kinetic study. Appl Catal A Gen. 451:127–136. doi:10.1016/j.apcata.2012.11.018.

Likozar B. 2011. Kinetic modeling of the peroxide cross-linking of polymer/monomer blends: from a theoretical model framework to its application for a complex polymer/monomer dispersion system. React Funct Polym. 71(1):11–22. doi:10.1016/j.reactfunctpolym.2010.11.004.

Likozar B, Krajnc M. 2011. Kinetic modeling of the peroxide cross-linking of polymers: from a theoretical model framework to its application for a complex polymer system. Chem Eng Process. 50(2):200–210. doi:10.1016/j.cep.2010.12.007.

Rahaman M, Graça NS, Pereira CSM, Rodrigues AE. 2015. Thermodynamic and kinetic studies for synthesis of the acetal (1,1-diethoxybutane) catalyzed by Amberlyst 47 ion-exchange resin. Chemical Engineering Journal. 264:258–267. doi:10.1016/j.cej.2014.11.077.

Rodriguez O, Setínek K. 1975. Dependence of Esterification Rates on Crosslinking of Ion Exchange Resins Used as Solid Catalysts. Praha-Suchdol. 39(3):449–455. doi:10.1016/0021-9517(75) 90312-7.

Russo V, Rossano C, Salucci E, Tesser R, Salmi T, Di Serio M. 2020. Intraparticle diffusion model to determine the intrinsic kinetics of ethyl levulinate synthesis promoted by Amberlyst-15. Chem Eng Sci. 228:115974. doi:10.1016/j.ces.2020.115974.

Sims MB. 2021. Controlled radical copolymerization of multivinyl crosslinkers: a robust route to functional branched macromolecules. Polym Int. 70(1):14–23. doi:10.1002/pi.6084.

Tejero MA, Ramírez E, Fité C, Tejero J, Cunill F. 2016. Esterification of levulinic acid with butanol over ion exchange resins. Appl Catal A Gen. 517:56–66. doi:10.1016/j.apcata.2016.02.032.

Tobita H. 2021. Gel point properties in batch free-radical vinyl/divinyl copolymerization. Macro Reaction Engineering. 15(6):1–11. doi:10.1002/mren.202100018.